Geochemical Perspectives Letters

Zirconium isotopic composition of the mantle through time

S.Y. Tian[1], F. Moynier[1*], E.C. Inglis[1], J. Creech[1,2], M. Bizzarro[1,3], J. Siebert[1,4], J.M.D. Day[1,5], I.S. Puchtel[6]

doi: 10.7185/geochemlet.2033

Abstract

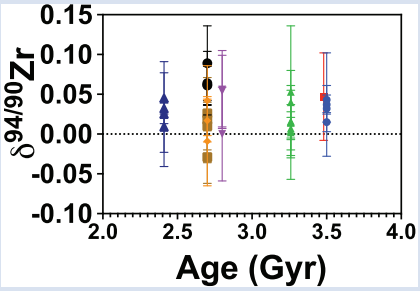

Zirconium isotopes have the potential to trace both magmatic differentiation and crustal evolution, as well as deep Earth processes. Zirconium is compatible in bridgmanite where it has a higher coordination number than in silicate melt, implying that Zr isotopes could be fractionated during magma ocean crystallisation. We report the Zr isotopic composition of 31 komatiites from around the globe, ranging in age from 2.41 to 3.55 Ga. The $\delta^{94/90}$Zr (*per* mille deviation of ^{94}Zr/^{90}Zr from IPGP-Zr standard) values for the komatiites are homogeneous at 0.030 ± 0.049 ‰ (all errors are 2 s.d.), and consistent with associated basaltic rocks (0.048 ± 0.032 ‰). These results, identical within uncertainty of the bulk silicate Earth estimate from modern basalts, suggest that the mantle Zr isotope composition has been constant since at least 3.55 Ga. Combining the isotopic compositions of komatiites and basalts of all ages we suggest a conservative $\delta^{94/90}$Zr = 0.040 ± 0.044 ‰ (n = 72) for the mantle composition. Several komatiite systems that we analysed in this study, including Schapenburg, Komati, and Weltevreden, have been previously argued to have isotope signatures consistent with magma ocean crystallisation processes. However, their Zr isotope compositions are indistinguishable from other komatiites, implying that bridgmanite crystallisation did not fractionate Zr isotopes to any measurable extent.

Received 19 May 2020 | Accepted 7 September 2020 | Published 7 October 2020

Introduction

Zirconium is a refractory element (Tc = 1741K; Lodders, 2003), and its abundance and stable isotopic composition is, *a priori*, robust to evaporation processes that occurred during planetary formation. This makes Zr distinct from more volatile elements, like Zn (Moynier *et al.*, 2017) or even Si and Mg (Pringle *et al.*, 2014; Hin *et al.*, 2017). As with other high field strength elements, Zr is lithophile and incompatible (Woodhead *et al.*, 1993; Johnson, 1998) and is enriched in the continental crust (Rudnick and Gao, 2003). Zirconium isotopes fractionate during magmatic differentiation. For example, the most evolved lavas from Hekla volcano, Iceland, have a ^{94}Zr/^{90}Zr ratio 0.5 ‰ higher than less evolved lavas. This is interpreted to reflect differences in coordination of zirconium between zircon and melt (Inglis *et al.*, 2019). Because of the resistance of zircons to physical and chemical abrasion and the availability of other isotope tracers (*e.g.*, O, Hf) and elements within them (*e.g.*, rare earth elements), they have found widespread application in the study of Earth's crust through time (Condie, 2005). The isotopic fractionation of Zr between granites and basalts (Inglis *et al.*, 2018) suggests that Zr isotopes could be used as tracers within zircons, and of crustal recycling in Earth's mantle, especially since Zr is a fluid immobile element and should be efficiently recycled into the mantle. Presently, the Zr isotopic composition of the mantle is estimated by the analysis of relatively low degree basaltic partial melts (Inglis *et al.*, 2019).

Komatiites are ultramafic volcanic rocks with >18 wt. % MgO. They are formed by partial melting in hot mantle plumes, mostly during the Archean (*e.g.*, Arndt *et al.*, 2008). Since komatiites are mantle-derived high degree partial melts (>30 %) (Herzberg, 1992), and Zr is moderately incompatible, almost all Zr from the mantle source is efficiently extracted into komatiitic melts. As such, komatiitic melts must faithfully reflect the Zr isotopic composition of their mantle source. Similar logic has been used to estimate the composition of the mantle through time of several other elements, including Ca (Amsellem *et al.*, 2019), Ga (Kato *et al.*, 2017), and Ti (Greber *et al.*, 2017; Deng *et al.*, 2018).

Komatiites span a range of ages and, thus, provide the potential to investigate initial mantle composition and, in particular, the processes of crystallisation of an early terrestrial magma ocean (Puchtel *et al.*, 2013, 2016b; Byerly *et al.*, 2017). For example, some komatiites from the Weltevreden formation in the Barberton Greenstone Belt, South Africa, have unusual Ca isotopic compositions compared with other komatiites and are interpreted as a record of mantle source heterogeneities induced

1. Université de Paris, Institut de Physique du Globe de Paris, CNRS, Paris, France
2. Department of Earth and Planetary Sciences, Macquarie University, NSW 2109, Australia
3. Centre for Star and Planet Formation, Globe Institute, University of Copenhagen, Copenhagen, Denmark
4. Institut Universitaire de France, Paris, France
5. Scripps Institution of Oceanography, University of California San Diego, La Jolla, CA 92093, USA
6. Department of Geology, University of Maryland, 8000 Regents Drive, College Park, MD 20742, USA
* Corresponding author (email: moynier@ipgp.fr)

by magma ocean crystallisation (Amsellem *et al.*, 2019). Zirconium is useful to search for traces of magma ocean crystallisation processes because it is compatible in bridgmanite ($D_{bridgmanite\text{-}melt} > 1$; Corgne *et al.*, 2005) and has different coordination numbers (CN) between bridgmanite (CN = 8, where it substitutes for Mg; Smyth and Bish, 1988), and silicate melt (CN = 6; Farges *et al.*, 1991). Since heavier isotopes tend to concentrate in the phases where it makes tighter bonds it is likely that crystallisation of bridgmanite from a melt would leave the residual liquid enriched in the heavier isotopes compared to bulk mantle.

Samples and Methods

Thirty one komatiite samples (olivine- and pyroxene-spinifex-textured and olivine cumulates) were studied (Table S-1). The komatiite samples are from Fennoscandia (Victoria's Lava Lake, Vetreny Belt; Kostomuksha Greenstone Belt), South Africa (Komati, Weltevreden, and Schapenburg Formations of the Barberton Greenstone Belt), Zimbabwe (Belingwe Greenstone Belt) and Canada (Boston Creek Flow, Abitibi Greenstone Belt and Munro Township). All samples have previously been studied for trace and highly siderophile element abundances, ^{186,187}Os, ^{142,143}Nd, ^{182}W isotope systematics (Puchtel *et al.*, 1998, 2001, 2005, 2009, 2013, 2016a,b), and for Ca stable isotopes (Amsellem *et al.*, 2019). Two widely available reference materials (BHVO-2 and AGV-2) for which Zr isotopic compositions have been reported previously (Inglis *et al.*, 2018; Tian *et al.*, 2020) were also analysed.

Given that komatiites have much lower Zr content than any previously analysed samples, we performed several full replicates (weighing, spike addition, dissolution, chemical separation, mass spectrometry analyses) (see Table S-1). These samples are noted "R" in Table S-1. The Zr isotopic composition was measured using a *ThermoFischer* Neptune plus MC-ICP-MS at the IPGP as described in Tian *et al.* (2020). The protocol utilised for Zr stable isotope measurements was adapted from Inglis *et al.* (2018) and is reported in Table S-2. The size of columns utilised had to be scaled up and the chemical purification method modified due to the high Ca/Zr of komatiites, and the associated risk of Zr coprecipitation with Mg, Ca fluorides (Tanaka *et al.*, 2003). To do this, the column procedure from Inglis *et al.* (2018) was reversed. The details of the analytical methods can be found in the Supplementary Information.

Results

The Zr isotopic compositions are reported in Table S-1 as:

$$\delta^{94/90}\mathrm{Zr} = \left[\frac{\left(\frac{^{94}\mathrm{Zr}}{^{90}\mathrm{Zr}}\right)_{\mathrm{sample}}}{\left(\frac{^{94}\mathrm{Zr}}{^{90}\mathrm{Zr}}\right)_{\mathrm{IPGP-Zr}}} - 1\right] \times 1000 \qquad \text{Eq. 1}$$

There is presently no international Zr isotopic standard commercially available and the majority of the Zr isotopic data for rock samples have been reported against the IPGP-Zr standard (calibrated against a variety of geostandards; Inglis *et al.*, 2018; Feng *et al.*, 2020; Guo *et al.*, 2020; Tian *et al.*, 2020). Alternatively, three other standards have been used: zircon GJ-1 for *in situ* analyses (Zhang *et al.*, 2019), an elemental Zr standard, NIST SRM3169 (Feng *et al.*, 2020) and a standard in development by NIST (Ibañez-Mejia and Tissot, 2019; Tompkins *et al.*, 2020) for bulk measurements. These three standards have been calibrated against the IPGP-Zr standard (Tian *et al.*, 2020).

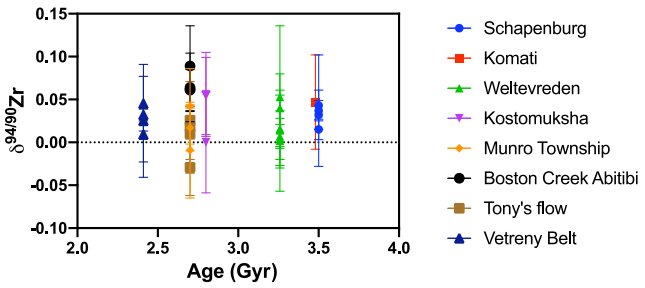

Figure 1 Zirconium isotopic composition of komatiites as a function of their crystallisation ages. The $\delta^{94/90}$Zr values are constant through 1 Ga and in various locations indicating that the terrestrial mantle had a constant $\delta^{94/90}$Zr value through time. The Weltevreden komatiites have unusual Ca isotope signatures consistent with magma ocean crystallisation processes. They do not have a different Zr isotopic composition from other komatiites. Errors as 2 s.d. of replicated measurements (typically 4).

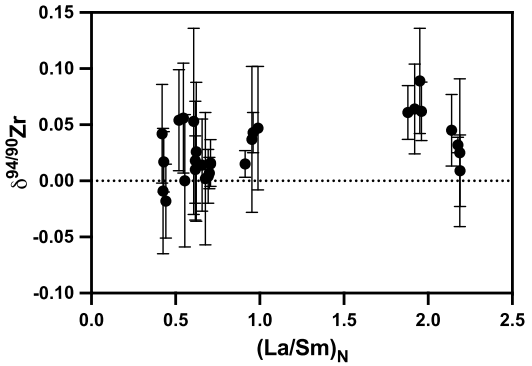

Figure 2 Zirconium isotopic composition of the komatiites as a function of the La/Sm ratio normalised to primitive mantle composition [$(La/Sm)_N$]. Variations in $(La/Sm)_N$ are interpreted to reflect prior melt extraction from komatiite source mantles. The absence of variation suggests that prior melt extraction did not fractionate Zr isotopes and that the source of the komatiites reflects the composition of the Archean mantle. Errors as 2 s.d. of the replicated measurements (typically 4).

The $\delta^{94/90}$Zr values of BHVO-2 (0.033 ± 0.025 ‰) and AGV-2 (0.017 ± 0.065 ‰) are consistent with the previous measurements obtained using a different chemical protocol ($\delta^{94/90}$Zr = 0.044 ± 0.044 ‰ and 0.044 ±0.050 ‰, respectively), (Inglis *et al.*, 2018) and the values reported in Tian *et al.* (2020) (0.045 ± 0.025 ‰ and 0.035 ± 0.037 ‰, respectively). Reproducibility of replicate analyses is consistent within the internal error defined by multiple replicate measurements of the same sample solutions. For example, the two replicates of SCH2.6 return a value of $\delta^{94/90}$Zr = 0.043 ± 0.018 ‰ (2 s.d.). In general, the Zr isotopic compositions of komatiites are relatively invariant, and show no correlation with age (Fig. 1) or the degree of prior melt removal (Fig. 2). The $\delta^{94/90}$Zr values of all the komatiites range from −0.018 to +0.089, with an average value of 0.030 ± 0.04 ‰ (2 s.d., n = 31).

Discussion

No measurable effects on Zr during magma ocean crystallisation. Based on Os, Nd, Hf, O and Ca isotopic compositions of some komatiites like Weltevreden it has been suggested that they

recorded the fractionation of minerals stable under magma ocean conditions (Puchtel *et al.*, 2013; Byerly *et al.*, 2017; Amsellem *et al.*, 2019). The source of these komatiites is enriched in the heavier isotopes of Ca, consistent with the extraction of light Ca in Ca perovskite into the lower mantle and the preservation of mantle heterogeneity until at least the extraction of the komatiites at 3.26 Ga (Amsellem *et al.*, 2019). Given the compatibility of Zr in bridgmanite and the CN differences between bridgmanite and silicate melt outlined previously, crystallisation of bridgmanite could fractionate Zr isotopes. The Weltevreden komatiites do not have anomalous Zr isotopic compositions (average $\delta^{94/90}$Zr value for Weltevreden is 0.019 ± 0.036 ‰, compared to 0.032 ± 0.054 ‰ for other komatiites; t test, p value = 0.19) and, therefore, cannot validate the hypothesis. Assuming magma ocean fractionation effects in the source of Weltevreden komatiites, the absence of Zr isotopic variations likely reflects limited bridgmanite-melt fractionation, because the difference in CN at high temperatures was insufficient to induce isotopic fractionation resolvable within analytical uncertainty.

Evolution of the Zr isotopic composition of Earth's mantle. The similarity (t test, p value = 0.56) of Zr isotope composition between spinifex-textured and chilled margin komatiites ($\delta^{94/90}$Zr = 0.027 ± 0.044 ‰, n = 14) and olivine cumulates ($\delta^{94/90}$Zr = 0.033 ± 0.054 ‰, n = 17; Table S-1) indicates that there was limited isotopic fractionation during komatiite crystallisation. This is illustrated by the absence of correlation between $\delta^{94/90}$Zr and Zr content (Fig. 3, R^2 = 0.2). Since komatiites are formed at temperatures >2000 K (Arndt *et al.*, 2008), isotopic fractionation during partial melting is minimised, and, therefore, they must represent the composition of their source. The sources of komatiites had been variably depleted by prior melt extractions, as evidenced from variations in the ratios of the light and heavy REE. This is exemplified by the normalised La/Sm ratio to the primitive mantle composition, $(La/Sm)_N$, that deviates from one. Prior melt extraction would also have extracted Zr from the source and, potentially, fractionated Zr isotopes. The komatiites analysed here encompass a large range of $(La/Sm)_N$ values, from 0.44 to 2.2 (Puchtel *et al.*, 1998, 2001, 2005; 2009, 2013, 2016a,b). The absence of correlation (R^2 = 0.2) between the $\delta^{94/90}$Zr values and $(La/Sm)_N$ (Fig. 2) indicates that the mantle sources of komatiites were not isotopically fractionated by prior melt extractions. The absence of temporal $\delta^{94/90}$Zr variations from 3.5 to 2.41 Ga (Fig. 1, R^2 = 0.004) provides further evidence that prior melt extraction did not change the Zr isotopic composition of the komatiite mantle sources.

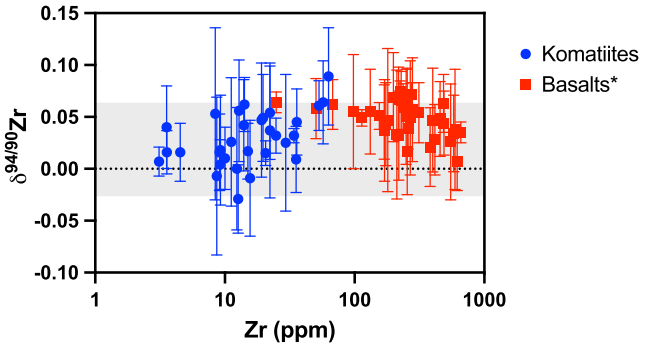

Figure 3 Zirconium isotopic composition of komatiites (this study) and basalts (literature) as a function of the Zr content of the samples. While Zr content varies over two orders of magnitude, the $\delta^{94/90}$Zr are consistent with an average value of 0.040 ± 0.044 (2 s.d., n = 72), which best reflects the composition of Earth's mantle (grey band). Errors as 2 s.d. of replicate measurements (typically 4). Data from Inglis *et al.* (2019).

Therefore, the average $\delta^{94/90}$Zr value of komatiites should reflect the composition of their mantle source. The average Zr isotopic composition of komatiites ($\delta^{94/90}$Zr = 0.030 ± 0.049 ‰) overlaps with the mantle's estimate based on young basaltic rocks ($\delta^{94/90}$Zr = 0.048 ± 0.032 ‰, Inglis *et al.*, 2019). When averaged together with the previously analysed basalts (Inglis *et al.*, 2019), a conservative estimate for the $\delta^{94/90}$Zr for the Earth's mantle of 0.040 ± 0.044 ‰ (2 s.d., n = 72) is calculated (grey band in Fig. 3). However, it should be noted that basalts are slightly lighter than komatiites (t test, p value = 0.001), which may indicate that low degree partial melt could be enriched in the heavier isotopes of Zr as previously suggested to explain the enrichments in light Zr isotopes in the mantle source of N-MORBs (Inglis *et al.*, 2019). Future analyses of mantle peridotites would allow further assessment of this issue.

Acknowledgements

We thank three anonymous reviewers and editor A. Shahar for their comments. SYT thanks support from CSC. FM acknowledges an ERC grant #637503. ISP thanks E. Nisbet, G. Byerly, and C. Anhaeusser for invaluable contributions to his komatiite collection.

Editor: Anat Shahar

Additional Information

Supplementary Information accompanies this letter at https://www.geochemicalperspectivesletters.org/article2033.

Cite this letter as: Tian, S.Y., Moynier, F., Inglis, E.C., Creech, J., Bizzarro, M., Siebert, J., Day, J.M.D., Puchtel, I.S. (2020) Zirconium isotopic composition of the mantle through time. *Geochem. Persp. Let.* 15, 40–43.

References

Amsellem, E., Moynier, F., Puchtel, I.S. (2019) Evolution of the Ca isotopic composition of the mantle. *Geochimica et Cosmochimica Acta* 258, 195–206.

Arndt, N., Lesher, M., Barnes, S. (2008) *Komatiite*. Cambridge University Press. Cambridge, New York, Melbourne.

Byerly, B.L., Kareem, K., Bao, H., Byerly, G.R. (2017) Early Earth mantle heterogeneity revealed by light oxygen isotopes of Archaean komatiites. *Nature Geoscience* 10, 871–875.

Condie, K.C. (2005) High field strength element ratios in Archean basalts: a window to evolving sources of mantle plumes? *Lithos* 79, 491–504.

Corgne, A., Liebske, C., Wood, B.J., Rubie, D.C., Frost, D.J. (2005) Silicate perovskite-melt partitioning of trace elements and geochemical signature of a deep perovskitic reservoir. *Geochimica et Cosmochimica Acta* 69, 485–496.

Deng, Z., Moynier, F., Sossi, P., Chaussidon, M. (2018) Bridging the depleted MORB mantle and the continental crust using titanium isotopes. *Geochemical Perspectives Letters* 9, 11–15.

Farges, F., Ponader, C.W., Brown Jr, G.E. (1991) Structural environments of incompatible elements in silicate glass/melt systems: I. Zirconium at trace levels. *Geochimica et Cosmochimica Acta* 55, 1563–1574.

Feng, L., Hu, W., Jiao, Y., Zhou, L., Zhang, W., Hu, Z., Liu, Y. (2020) High-precision stable zirconium isotope ratio measurements by double spike thermal ionization mass spectrometry. *Journal of Analytical Atomic Spectrometry* 35, 736–745.

Greber, N.D., Dauphas, N., Puchtel, I.S., Hofmann, B.A., Arndt, N.T. (2017) Titanium stable isotopic variations in chondrites, achondrites and lunar rocks. *Geochimica et Cosmochimica Acta* 213, 534–552.

Guo, J.L., Wang, Z., Zhang, W., Moynier, F., Cui, D., Hu, Z., Ducea, M. (2020) Significant Zr isotope variations in single zircon grains recording magma evolution history. *Proceedings of the National Academy of Sciences*, doi: 10.1073/pnas.2002053117.

Herzberg, C. (1992) Depth and degree of melting of komatiite. *Journal of Geophysical Research* 97, 4521–4540.

Hin, R.C., Coath, C.D., Carter, P.J., Nimmo, F., Lai, Y.J., Pogge von Strandmann, P.A.E., Willbold, M., Leinhardt, Z.M., Walter, M.J., Elliott, T. (2017) Magnesium isotope evidence that accretional vapour loss shapes planetary compositions. *Nature* 549, 511–515.

Ibañez-Mejia, M., Tissot, F.L. (2019) Extreme Zr stable isotope fractionation during magmatic fractional crystallization. *Science Advances* 5, eaax8648.

Inglis, E.C., Creech, J.B., Deng, Z., Moynier, F. (2018) High-precision zirconium stable isotope measurements of geological reference materials as measured by double-spike MC-ICPMS. *Chemical Geology* 493, 544–552.

Inglis, E., Moynier, F., Creech, J., Deng, Z., Day, J.M.D., Teng, F.-Z., Bizzarro, M., Jackson, M.J., Savage, P. (2019) Isotopic fractionation of zirconium during magmatic differentiation and the stable isotope composition of the silicate Earth. *Geochimica et Cosmochimica Acta* 250, 311–323.

Johnson, K.T. (1998) Experimental determination of partition coefficients for rare earth and high-field-strength elements between clinopyroxene, garnet, and basaltic melt at high pressures. *Contributions to Mineralogy and Petrology* 133, 60–68.

Kato, C., Moynier, F., Foriel, J., Teng, F., Puchtel, I.S. (2017) The gallium isotopic composition of the bulk silicate Earth. *Chemical Geology* 448, 164–172.

Lodders, K. (2003) Solar System abundances and condensation temperatures of the elements. *Astrophysical Journal* 591, 1220–1247.

Moynier, F., Vance, D., Fujii, T., Savage, P. (2017) The isotope geochemistry of copper and zinc. In: Teng, F.-Z., Watkins, J., Dauphas, N. (Eds.) *Reviews in Mineralogy & Geochemistry* 82, 543–600.

Pringle, E.A., Moynier, F., Savage, P.S., Badro, J., Barrat, J.A. (2014) Silicon isotopes in angrites and volatile loss in planetesimals. *Proceedings of the National Academy of Science USA* 111, 17029–32.

Puchtel, I., Hofmann, A., Mezger, K., Jochum, K., Shchipansky, A., Samsonov, A. (1998) Oceanic plateau model for continental crustal growth in the Archaean: a case study from the Kostomuksha greenstone belt, NW Baltic Shield. *Earth and Planetary Science Letters* 155, 57–74.

Puchtel, I.S., Brügmann, G.E., Hofmann, A.W. (2001) ^{187}Os-enriched domain in an Archean mantle plume: evidence from 2.8 Ga komatiites of the Kostomuksha greenstone belt, NW Baltic Shield. *Earth and Planetary Science Letters* 186, 513–526.

Puchtel, I.S., Brandon, A.D., Humayun, M., Walker, R.J. (2005) Evidence for the early differentiation of the core from Pt–Re–Os isotope systematics of 2.8-Ga komatiites. *Earth and Planetary Science Letters* 237, 118–134.

Puchtel, I., Walker, R., Brandon, A., Nisbet, E. (2009) Pt–Re–Os and Sm–Nd isotope and HSE and REE systematics of the 2.7Ga Belingwe and Abitibi komatiites. *Geochimica et Cosmochimica Acta* 73, 6367–6389.

Puchtel, I., Blichert-Toft, J., Touboul, M., Walker, R., Byerly, G., Nisbet, E., Anhaeusser, C. (2013) Insights into early Earth from Barberton komatiites: evidence from lithophile isotope and trace element systematics. *Geochimica et Cosmochimica Acta* 108, 63–90.

Puchtel, I., Touboul, M., Blichert-Toft, J., Walker, R., Brandon, A., Nicklas, R., Kulikov, V., Samsonov, A. (2016a) Lithophile and siderophile element systematics of Earth's mantle at the Archean–Proterozoic boundary: evidence from 2.4Ga komatiites. *Geochimica et Cosmochimica Acta* 180, 227–255.

Puchtel, I.S., Blichert-Toft, J., Touboul, M., Horan, M.F., Walker, R.J. (2016b) The coupled ^{182}W-^{142}Nd record of early terrestrial mantle differentiation. *Geochemistry, Geophysics, Geosystems* 17, 2168–2193.

Rudnick, R.L., Gao, S. (2003) Composition of the Continental Crust. In: Holland, H.D., Turekian, K.K. (Eds.) *Treatise on Geochemistry* 3, 1–64.

Smyth, J.R., Bish, D.L. (1988) *Crystal structures and cation sites of the rock-forming minerals*. Allen & Unwin, Boston.

Tanaka, R., Makishima, A., Kitagawa, H., Nakamura, E. (2003) Suppression of Zr, Nb, Hf and Ta coprecipitation in fluoride compounds for determination in Ca-rich materials. *Journal of Analytical Atomic Spectrometry* 18, 1458–1463.

Tian, S., Inglis, E., Creech, J., Zhang, W., Wang, Z., Hu, Z., Liu, Y., Moynier, F. (2020) The zirconium stable isotope compositions of 22 geological reference materials, 4 zircons and 3 standard solutions. *Chemical Geology*, doi: 10.1016/j.chemgeo.2020.119791.

Tompkins, H., Zieman, L., Ibanez-Mejia, M., Tissot, F. (2020) Zirconium stable isotope analysis of zircon by MCICP-MS:methods and application to evaluating intra-crystalline zonation in a zircon megacryst. *Journal of Analytical Atomic Spectrometry*, doi: 10.1039/c9ja00315k.

Woodhead, J., Eggins, S., Gamble, J. (1993) High field strength and transition element systematics in island arc and back-arc basin basalts: evidence for multi-phase melt extraction and a depleted mantle wedge. *Earth and Planetary Science Letters* 114, 491–504.

Zhang, W., Wang, Z., Moynier, F., Inglis, E., Tian, S., Li, M., Liu, Y., Hu, Z. (2019) Determination of Zr isotopic ratios in zircons using laser-ablation multiple-collector inductively coupled-plasma mass-spectrometry. *Journal of Analytical Atomic Spectrometry* 34, 1800–1809.

Geochemical Perspectives Letters

Zirconium isotopic composition of the mantle through time

S.Y. Tian, F. Moynier, E.C. Inglis, J. Creech, M. Bizzarro, J. Siebert, J.M.D. Day, I.S. Puchtel

Supplementary Information

The Supplementary Information includes:

- Methods
- Tables S-1 to S-3
- Supplementary Information References

Methods

Homogenous sample powders were aliquoted in order to obtain a minimum of 1 µg Zr per sample. This equated to a few 100s mg of powder in most cases. The aliquots were then spiked with a ^{91}Zr–^{96}Zr double-spike (51.4% ^{91}Zr and 48.6% ^{96}Zr) at an optimal spike to sample ratio of 43:57 prior to sample digestion (Inglis *et al.*, 2018). The sample powders were digested in Parr bombs using a mixture of concentrated HF and HNO_3 at a 3:1 (v/v) ratio to ensure full dissolution (see Inglis *et al.*, 2018). The samples were then dried down and dissolved in 2 mL of 6M HCl at 140 °C for one day, evaporated to dryness and further dissolved in 2 mL using a mixture of HCl (~6M) and HNO_3 (~16M) at a 3:1 (v/v) ratio at 120°C for one day. After this the solutions were visually checked to ensure that full dissolution was achieved. The protocol utilized for Zr stable isotope measurements here was adapted from Inglis *et al*. (2018) and is reported in Table S-2. We first had to increase the volume of the acid utilised in Inglis *et al*. (2018) for high Zr samples (*e.g*. basalts, zircons) to accommodate for the larger amount of sample loaded onto the columns. We also modified the protocol of chemical purification to take into account the high Ca/Zr ratio of komatiites compared to basalts, and the associated risk of Zr coprecipitation with Mg-Ca fluorides (Tanaka *et al.*, 2003). To do this we simply reverse the order of the two columns from Inglis *et al*. (2018) in order to remove Ca and Mg.

The full protocol included a first clean up of Fe using an AG1-X8 column with solutions as 6M HCl. The purified solutions were then dried down. Subsequently they were treated with 16M HNO_3 and evaporated to dryness before being loaded on 1 mL Eichrom DGA resin in 1 mL of 12M HNO_3. Elements including Ca, Fe, Ti and Mo were eluted with 12 mL of 12M HNO_3 and 12 mL 3M HNO_3 in sequence. Following this the Zr was eluted from the column in 10mL of a mixture HNO_3 (3M) and HF (0.2M). After evaporation of the Zr cut, the samples were loaded on a 2 mL anion exchange resin (Bio-Rad AG1-X8 200-400 mesh) in 4M HF. The matrix is eluted with 32 mL of 4M HF, apart

from Hf, Te and W which remain on the resin along with Zr (Schönbächler *et al.*, 2004). The remaining Zr were collected using 10 mL of a mixture of 6M HCl and 0.01M HF.

After purification, sample solutions were dried down and then treated with 16M HNO_3 at 100 °C for 2 hours to remove any potential organic residues eluted from the resin. Finally, the Zr cut was dried down and dissolved in a mixture of HNO_3 (0.5M) and HF (0.1M) for analysis.

The Zr isotopic composition was measured using a *Thermo Fisher* Neptune plus multi-collector inductively coupled plasma mass spectrometer (MC-ICP-MS) at the Institut de Physique du Globe de Paris, France, as described in Tian *et al.* (2020) and adapted from Inglis *et al.* (2018). The details of the instrumental operating parameters are given in Table S-3. Data acquisition consisted of 1 block of 50 cycles with integration time of 4.194 seconds. Washouts consisting of 7 minutes in 1M HNO_3 + 0.1M HF were conducted after every analysis, and baselines were measured on-peak prior to each analysis, comprising one block of 10 x 4.194 s integrations in 0.5M HNO3 + 0.1M HF. Ion beams from ^{90}Zr, ^{91}Zr, ^{92}Zr, ^{94}Zr, ^{95}Mo and ^{96}Zr were collected simultaneously in a static configuration using Faraday cups connected to 10^{11} Ω amplifiers. Three isotopic ratios are required in the double-spike equations to solve for the three unknowns: 1) mass-dependent fractionation factors of samples relative to the standard, 2) the instrumental fractionation factor and 3) the mass fraction of the Zr contributed from the double spike in the sample–double spike mixture. The Zr isotope ratios $^{91}Zr^+/^{90}Zr^+$, $^{94}Zr^+/^{90}Zr^+$ and $^{96}Zr^+/^{90}Zr^+$ were used for double spike data inversion calculation, which was achieved using the *IsoSpike* addon for the software package *Iolite* (Creech and Paul, 2015). The potential presence of Mo was monitored using mass $^{95}Mo^+$, and Mo interferences were corrected assuming the natural Mo isotope composition from Berglund and Wieser (2011) corrected for instrumental mass bias. Natural Mo isotope ratios were corrected using the instrumental mass bias determined from the double-spike calculations, and the calculated ^{92}Mo, ^{94}Mo and ^{96}Mo were subtracted from the signals of ^{92}Zr, ^{94}Zr and ^{96}Zr, respectively, prior to calculation of raw ratios; this procedure was repeated such that the mass bias (and, thus, corrected ratios) converged on a constant value.

Supplementary Tables

Table S-1 Zirconium isotopic composition of 31 komatiites and of two geological reference materials. The data are reported as $\delta^{94/90}$Zr, the per mil deviation of the ^{94}Zr/^{90}Zr from the IPGP-Zr standard. "R" denotes full replicates of the sample measurements. Zr concentrations are calculated by isotope dilution. "n" are the number of replicates.

Sample name	Location	Age Ga	Texture	$\delta^{94/90}$Zr	2SD	Zr (ppm)	n
SCH1.6	Schapenburg, South Africa (SA)	3.55	Ol-spinifex	0.032	0.017	24.8	8
SCH2.1	Schapenburg, SA	3.55	Ol-spinifex	0.015	0.012	20.6	4
SCH2.6	Schapenburg, SA	3.55	Ol-spinifex	0.049	0.042	19.7	4
SCH2.6-R	Schapenburg, SA	3.55	Ol-spinifex	0.036	0.030	23.4	8
SCH2.6 average	Schapenburg, SA	3.55	Ol-spinifex	0.043	0.018	21.5	2
SCH3.6	Schapenburg, SA	3.55	Ol-spinifex	0.037	0.065	22.3	4
BV10	Komati, Barberton, SA	3.48	Ol-cumulate	0.047	0.055	19.2	4
12-2	Weltevreden, Barberton, SA	3.26	Ol-spinifex	0.004	0.024	9.2	2
12-6	Weltevreden, Barberton, SA	3.26	Ol-cumulate	0.007	0.014	3.1	4
12-8	Weltevreden, Barberton, SA	3.26	Ol-cumulate	0.016	0.028	4.5	4
12-8-R	Weltevreden, Barberton, SA	3.26	Ol-cumulate	0.014	0.01	4.3	6
12-8 average	Weltevreden, Barberton, SA	3.26	Ol-cumulate	0.015	0.003	4.4	2
501-1	Weltevreden, Barberton, SA	3.26	Ol-cumulate	0.016	0.021	3.6	6
564-2	Weltevreden, Barberton, SA	3.26	Ol-cumulate	0.040	0.040	3.6	4
564-4	Weltevreden, Barberton, SA	3.26	Ol-spinifex	0.016	0.037	9.1	2
564-4-R	Weltevreden, Barberton, SA	3.26	Ol-spinifex	-0.007	0.076	8.7	4
564-4-R	Weltevreden, Barberton, SA	3.26	Ol-spinifex	0.034	0.032	6.9	8
564-4 average	Weltevreden, Barberton, SA	3.26	Ol-spinifex	0.014	0.041	8.2	3
564-5	Weltevreden, Barberton, SA	3.26	Ol-spinifex	0.002	0.059	8.7	2
564-6	Weltevreden, Barberton, SA	3.26	Chilled margin	0.053	0.083	8.4	2
94100	Kostomuksha, Baltic Shield	2.8	Ol-cumulate	0.056	0.049	12.9	4
94126	Kostomuksha, Baltic Shield	2.8	Ol-cumulate	0.000	0.059	12.4	4
9497	Kostomuksha, Baltic Shield	2.8	Ol-spinifex	0.054	0.045	22.3	4
PH26	Pyke Hill, Canada	2.7	Ol-spinifex	0.042	0.044	14.0	2
PH27	Pyke Hill, Canada	2.7	Ol-spinifex	-0.009	0.056	15.6	4
PH28	Pyke Hill, Canada	2.7	Ol-spinifex	0.017	0.027	15.1	4
BC02	Boston Creek, Canada	2.7	Px-spinifex	0.064	0.040	57.2	4

BC03	Boston Creek, Canada	2.7	Px-spinifex	0.089	0.047	62.9	4
BC06	Boston Creek, Canada	2.7	Ol-cumulate	0.061	0.024	53.2	4
BC08	Boston Creek, Canada	2.7	Ol-cumulate	0.062	0.026	14.2	4
ZV10	Tony's flow, Zimbabwe	2.7	Ol cumulate	-0.029	0.033	12.7	4
ZV10-R	Tony's flow, Zimbabwe	2.7	Ol cumulate	-0.006	0.078	11.4	4
ZV10 average	Tony's flow, Zimbabwe	2.7	Ol cumulate	-0.018	0.033	12.0	2
TN17	Tony's flow, Zimbabwe	2.7	Ol cumulate	0.010	0.030	10.0	4
TN18	Tony's flow, Zimbabwe	2.7	Ol cumulate	0.018	0.053	9.3	4
TN19	Tony's flow, Zimbabwe	2.7	Ol cumulate	0.026	0.062	11.2	4
01001	Vetreny Belt, Baltic Shield	2.41	Ol-cumulate	0.035	0.050	34.1	4
01001-R	Vetreny Belt, Baltic Shield	2.41	Ol-cumulate	0.030	0.013	34.0	4
01001 average	Vetreny Belt, Baltic Shield	2.41	Ol-cumulate	0.032	0.007	34.0	2
01104	Vetreny Belt, Baltic Shield	2.41	Ol-cumulate	0.009	0.032	35.4	4
01104-R	Vetreny Belt, Baltic Shield	2.41	Ol-cumulate	0.035	0.039	36.0	4
01104 average	Vetreny Belt, Baltic Shield	2.41	Ol-cumulate	0.022	0.037	35.7	2
01105	Vetreny Belt, Baltic Shield	2.41	Ol-cumulate	0.025	0.066	29.5	4
01106	Vetreny Belt, Baltic Shield	2.41	Ol-cumulate	0.045	0.032	35.8	4
BHVO-2	USGS GRM			0.033	0.025	155.6	4
AGV-2	USGS GRM			0.017	0.065	238.7	4

Table S-2 Zirconium chemical purification protocol.

First stage. AG1-X8 (2 mL, 200–400 mesh)		
Step	Reagent	Volume(mL)
Resin cleaning	2M HNO_3	8
	MQ H_2O	8
Conditioning	6 M HCl	8 (4*2)
Sample load and Zr collection	6 M HCl	8 (2+6)
Second stage. DGA (1.4 mL, 200–400 mesh)		
Step	Reagent	Volume(mL)
Resin cleaning	MQ H_2O	6
	12 M HNO_3	6
	3 M HNO_3 + 0.2 M HF	6
Conditioning	12 M HNO_3	8 (4*2)
Sample load	12 M HNO_3	1
Matrix elution	12 M HNO_3	12 (6*2)
	3 M HNO_3	12 (6*2)
Zr collection	3 M HNO_3 + 0.2 M HF	10 (5*2)
Third stage. AG1-X8 (2 mL, 200–400 mesh)		
Step	Reagent	Volume(mL)
Resin cleaning	2M HNO_3	6
	MQ H_2O	6
	6M HCl + 0.01M HF	6
	MQ H_2O	2
Conditioning	4 M HF	8 (4*2)
Sample load	4 M HF	2
Matrix elution	4 M HF	32 (8*4)
Zr collection	6M HCl +0.01M HF	10 (5*2)

Table S-3 MC-ICP-MS operation parameters for Zr isotope measurements.

Neptune Plus MC-ICP-MS	
RF power	1200 W
Cool gas flow	16 L min^{-1}
Auxiliary gas flow	~ 1 L min^{-1}
Sample gas flow	~ 1 L min^{-1}
Argon make-up gas flow (only CSC Mode)	0.29 ~ 0.34 L min^{-1}
Cones	Ni Jet cone, Ni 'H' cone
Mass resolution mode	Low ($M/\Delta M \approx 1700$)
Acceleration voltage	10 kV
Mass analyzer pressure	~ 8 x 10^{-9} mbar
Introduction System	PFA cyclonic spray chamber
Sample uptake rate	~ 50 mL min^{-1}
Solution running concentration	200 ng mL^{-1}
Typical sensitivity	~ 9 V
Integration time	4.194 s
Cycle numbers per analysis	50
Washout time	7 min
Faraday cup Configuration	
L2	^{90}Zr
L1	^{91}Zr
C	^{92}Zr
H2	^{94}Zr
H3	^{95}Mo
H4	^{96}Zr

Supplementary Information References

Berglund, M., Wieser, M.E. (2011) Isotopic compositions of the elements 2009 (IUPAC Technical Report). *Pure and Applied Chemistry* 83, 397–410.

Creech, J.B., Paul, B. (2015) IsoSpike: Improved Double-Spike Inversion Software. *Geostandards and Geoanalytical Research* 39, 7-15.

Inglis, E.C., Creech, J.B., Deng, Z., Moynier, F. (2018) High-precision zirconium stable isotope measurements of geological reference materials as measured by double-spike MC-ICPMS. *Chemical Geology* 493, 544-552.

Schönbächler, M., Rehkämper, M., Lee, D.-C., Halliday, A.N. (2004) Ion exchange chromatography and high precision isotopic measurements of zirconium by MC-ICP-MS. *Analyst* 129, 32-37.

Tanaka, R., Makishima, A., Kitagawa, H., Nakamura, E. (2003) Suppression of Zr, Nb, Hf and Ta coprecipitation in fluoride compounds for determination in Ca-rich materials. *Journal of Analytical Atomic Spectrometry* 18, 1458-1463.

Tian, S., Inglis, E., Creech, J., Zhang, W., Wang, Z., Hu, Z., Liu, Y., Moynier, F. (2020) The zirconium stable isotope compositions of 22 geological reference materials, 4 zircons and 3 standard solutions. *Chemical Geology*, doi: 10.1016/j.chemgeo.2020.119791.